sustainability

MDPI

Article

A Comprehensive Assessment of the Economic Performance of an Innovative Solar Thermal System: A Case Study

Lisa Gobio-Thomas [1], Mohamed Darwish [2], Antonio Rovira [3], Ruben Abbas [4], Magdalena Barnetche [4], Juan Pedro Solano [5], Albert Torres [6], Krzysztof Naplocha [7], Peter Kew [8] and Valentina Stojceska [1,9,*]

1 Department of Mechanical and Aerospace Engineering, College of Engineering Design and Physical Sciences, Brunel Univeristy London, Kingston Lane, Uxbridge UB8 3PH, UK; lisa.gobio-thomas@brunel.ac.uk
2 Department of Electronic & Electrical Engineering, College of Engineering Design and Physical Sciences, Brunel Univeristy London, Kingston Lane, Uxbridge UB8 3PH, UK; mohamed.darwish@brunel.ac.uk
3 Depatment of Energy Engineering, Universidad Nacional de Educación a Distancia (UNED), Juan del Rosal 12, 28040 Madrid, Spain; rovira@ind.uned.es
4 ETSI Industriales, Universidad Politécnica de Madrid (UPM), José Gutiérrez Abascal 2, 28006 Madrid, Spain; ruben.abbas@upm.es (R.A.); m.barnetche@upm.es (M.B.)
5 Depatment of Energy Engineering, Universidad Politécnica de Cartagena (UPCT), Edif. La Milagrosa, 30202 Cartagena, Spain; juanp.solano@upct.es
6 IRIS Technology, Carretera d'Esplugues 39-41, Cornellà de Lobregat, 08940 Barcelona, Spain; albert.torres@iris-eng.com
7 Department of Lightweight Elements Engineering, Foundry and Automation, Wroclaw University of Science & Technology, ul. Smoluchowskiego 25, 50-371 Wroclaw, Poland; krzysztof.naplocha@pwr.edu.pl
8 David Reay & Associates, P.O. Box 25, Whitley Bay, Tyne & Wear NE26 1QT, UK; p.a.kew@hw.ac.uk
9 Institute of Energy Futures, Centre for Sustainable Energy Use in Food Chains, Brunel University London, Kingston Lane, Uxbridge UB8 3PH, UK
* Correspondence: valentina.stojceska@brunel.ac.uk

Abstract: An economic assessment of an innovative solar thermal system called Application to Solar Thermal Energy to Processes (ASTEP) was conducted. It considered its three main subsystems: a novel rotary Fresnel SunDial, Thermal Energy Storage (TES) and Control System. Current Fresnel collectors are unable to provide thermal energy above 150 °C in high-latitude locations. Therefore, the key contribution of this study is the assessment of the economic performance of the ASTEP system used to provide high-temperature process heat up to 400 °C for industries located at low and high latitudes. The ASTEP system is installed at two end-users: Mandrekas (MAND), a dairy factory located in Greece at a latitude of 37.93 N and ArcelorMittal (AMTP), a manufacturer of steel tubes located in Romania at a latitude of 47.1 N. The life cycle costs (LCC), levelised cost of energy (LCOE), energy cost savings, EU carbon cost savings and benefit–cost ratio (BCR) of the ASTEP system were assessed. The results showed that AMTP's ASTEP system had higher LCC and LCOE than MAND. This can be attributed to the use of two TES tanks and a double-axis solar tracking system for AMTP's ASTEP system due to its high latitude location, compared to a single TES tank and single-axis solar tracking system used for MAND at low latitude. The total financial savings of the ASTEP system were EUR 249,248 for MAND and EUR 262,931 for AMTP over a period of 30 years. This study demonstrates that the ASTEP system offers financial benefits through its energy and EU carbon cost savings for industries at different latitudes while enhancing their environmental sustainability.

Keywords: economic assessment; life cycle costing (LCC); solar thermal systems; capital costs; levelised cost of energy (LCOE); sustainability; benefit–cost ratio; energy cost savings; carbon cost savings

check for updates

Academic Editor: Kian Jon Chua

Received: 20 October 2024
Revised: 18 December 2024
Accepted: 20 December 2024
Published: 9 January 2025

Citation: Gobio-Thomas, L.; Darwish, M.; Rovira, A.; Abbas, R.; Barnetche, M.; Solano, J.P.; Torres, A.; Naplocha, K.; Kew, P.; Stojceska, V. A Comprehensive Assessment of the Economic Performance of an Innovative Solar Thermal System: A Case Study. *Sustainability* **2025**, *17*, 455. https://doi.org/10.3390/su17020455

1. Introduction

Demand for energy has risen significantly over the years due to population growth and socio-economic development. This energy demand has predominately been met through the use of fossil fuels, which causes negative environmental impacts such as global warming, air pollution and health issues like asthma and other respiratory illnesses. These concerns have placed environmental sustainability at the forefront of government and international policies. In line with this, the United Nations Framework Convention on Climate Change and the 2015 Paris Agreement set the ambitious goals of limiting global warming to 1.5 °C to prevent extreme climate change impacts, including more frequent and severe droughts, heatwaves and rainfall [1]. In order to fulfil this international climate change mandate, the EU and its member states have agreed to reduce their GHG emissions by at least 55% by 2030 and achieve climate neutrality by 2050 [2]. To support this transition, the EU has provided a number of incentives to increase the development and use of renewable energy technologies in various sectors to reduce the dependence on fossil fuels and their GHG emissions [3]. Among the renewable energy technologies receiving increased scientific and commercial attention is concentrating solar power, also known as solar thermal technologies [4]. These systems include parabolic trough (PT), solar tower (ST), solar dish (SD) and linear Fresnel (LFR). Over the years, the use of solar energy for heating and cooling in industrial processes has increased, highlighting the growing interest of the industry in improving their environmental sustainability. Most of the solar thermal technologies currently used in EU industries provide thermal energy below 150 °C [5]. However, in order to replace fossil fuels consumption, solar thermal technologies must be capable of producing heat above 150 °C, as most of the thermal energy requirements for industrial processes exceed this threshold [5].

As a result, a new system called ASTEP has been developed to provide thermal energy up to 400 °C [6]. The novelty of the ASTEP system lies in its SunDial, which consists of a rotary platform with a number of short, parallel Fresnel collectors mounted on top and uses a two-axis tracking system to capture more solar irradiance to deliver high-temperature thermal energy in high-latitude regions, where conventional Fresnel solar thermal systems fail to meet thermal energy needs [5,7].

While several studies have been conducted on the economic assessment of solar thermal technologies [8–12], the majority have been centred on PT and ST solar thermal plants used for electricity generation. Hirbodi et al. [9] and Aseri et al. [10] assessed the economic performance of PT and ST solar thermal plants using capital costs and LCOE metrics. The results showed that the ST plants had lower capital costs and LCOE than the PT plants. However, the life cycle costs (LCC) and benefit–cost ratio (BCR) of these plants were not calculated which is important to understand the long-term economic performance of the plants. This highlights the need for studies on the economic performance of solar thermal plants with smaller capacity used to provide thermal energy for industries. This study addresses this gap by presenting the first LCC analysis of solar thermal systems specifically designed to deliver thermal energy to industrial processes across various latitudes. In the reviewed literature, the only study found that assessed both the internal and external economic performance was based on a PT solar thermal plant used only for electricity generation rather than for providing thermal energy to industries [4]. The internal costs are all the costs incurred during the life span of the plant such as the capital costs, LCC and LCOE. The external costs are the costs associated with atmospheric emissions throughout the plant's life cycle, such as the EU carbon costs. To the best of the authors' knowledge, this is also the first study to evaluate both the internal and external economic performance of a Fresnel solar thermal system.

1.1. *Description of ASTEP System*

ASTEP consists of three main subsystems, which are the SunDial, Thermal Energy Storage and Controls (Figure 1). It has been designed to provide thermal energy up to 400 °C to industries located at both high and low latitudes [6]. It is applied to two end-users located at different latitudes in Romania and Greece (Figure 2). The first one is Mandrekas (MAND), a dairy factory located in Greece at a latitude of 37.93 N, and the second is ArcelorMittal (AMTP), a manufacturer of steel tubes located in Romania at a latitude of 47.1 N. MAND requires thermal energy of 175 °C to pasteurise milk and ferment yoghurt and has a cooling demand of 5 °C to refrigerate their products. AMTP requires thermal energy above 220 °C for the pre-heating of the steel tubes before colour coating is applied to the tubes [6].

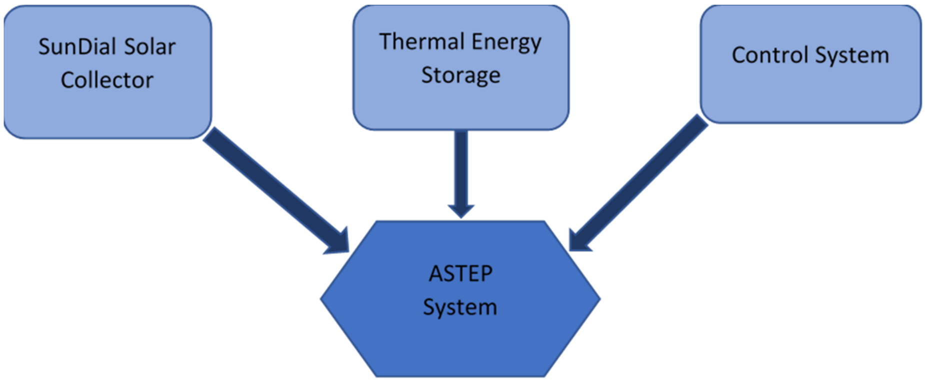

Figure 1. Main components of ASTEP system.

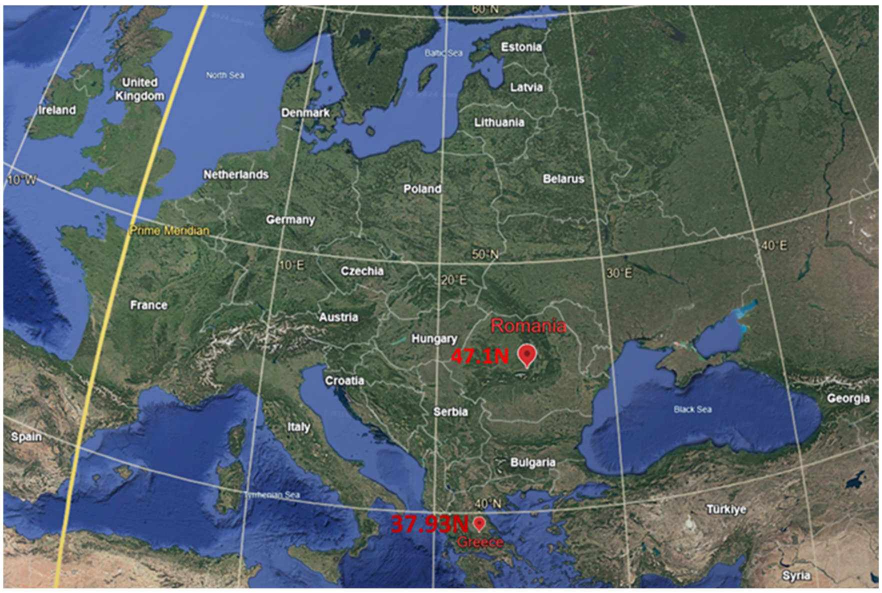

Figure 2. Map of Europe displaying location of Romania and Greece (GoogleEarth).

The closer the location is to the equator at low latitude, the higher its local irradiance (Figure 2). Therefore, Greece which is located at low-latitude has a higher local irradiance than Romania. Furthermore, the average DNI in Corinth, Greece, where MAND is located, is higher at 464 W/m^2 compared to 417 W/m^2 for Iasi, Romania, where AMTP is located [13].

1.1.1. SunDial Solar Collector

The SunDial solar collector is the first part of the ASTEP system (Figure 1) and consists of short, parallel Fresnel collectors installed on top of a rotary platform that tracks the sun. The novelty of the SunDial is that it can operate at low latitudes as well as high-latitude regions where current Fresnel collectors are unable to provide thermal energy above 150 °C [5]. Two unique designs of the SunDial have been developed to operate at low-latitude and high-latitude locations, as follows:

- Low-latitude Design: This SunDial design consists of a single-axis tracking system, where only the platform rotates to capture solar irradiance, whilst the mirrors are stationary on the platform. This results in easy and quick installation and maintenance of the system. To reduce the cosine and end losses of the SunDial and improve its efficiency, the mirror field is tilted longitudinally and the mirrors are shorter than the receivers, with the lateral mirrors shorter than the central mirrors [13]. This design has been implemented for MAND and is illustrated in Figure 3a.
- High-latitude Design: This SunDial design consists of a double-axis tracking system, where the platform rotates to maintain the sun within the field's cross-section, resulting in a significant reduction in cosine losses. Each of the SunDial's mirrors must also rotate to track the sun's varying elevation as the cross-section sun altitude changes through the day. The mirror's axes and receivers are located in two tilted planes, to minimise shading losses. This SunDial design has been developed to accommodate high-latitude regions, as the sun's altitude is low for most of the year [13]. This design has been implemented for AMTP and is illustrated in Figure 3b.

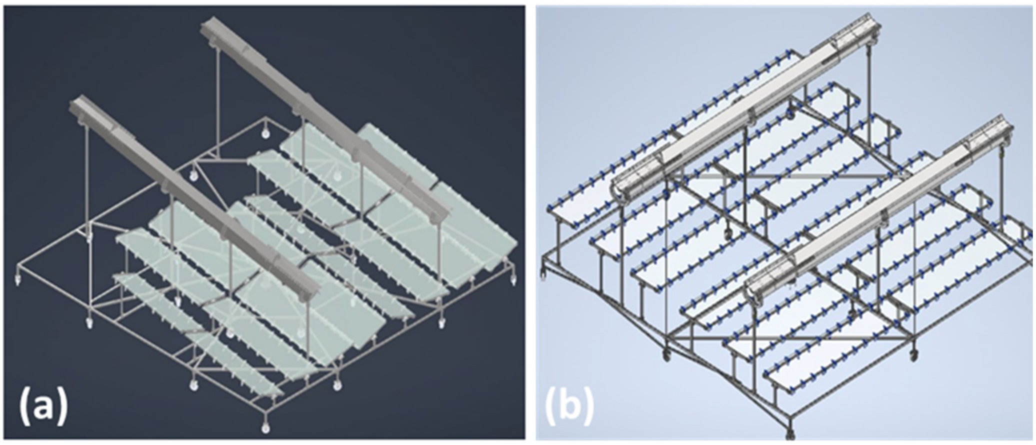

Figure 3. Design of SunDial concentrators for (**a**) Mandrekas–37.93 N and (**b**) ArcelorMittal–47.1 N [7] (reproduced with permission of the Editor-in-Chief of *Thermal Science and Engineering Progress*).

1.1.2. Thermal Energy Storage

The thermal energy storage (TES) that is the second part of the ASTEP system (Figure 1), is based on phase change materials (PCM) with a multi-component mixture of sodium and potassium nitrate salts ($NaNO_3$-KNO_3) as the PCM material. The TES tank (Figure 4a) stores excess solar thermal energy produced by the Sundial during peak production hours, and delivers it to the end user when it is required. The passive design of the TES consists of honeycomb structures which are in a shell enclosure and have the form of multi tubes with integrated elements enhancing the heat transfer. The heat transfer fluid (HTF) flows through the inside tubes, and the PCM is stored at the shell side (Figure 4b), filling the structure created by the honeycomb. This active design makes it possible to control the stored thermal energy during charging and to release it during discharging [7]. The TES is used by both end users, MAND and AMTP. A single TES tank was used for MAND's

ASTEP system due to its low latitude location, while two TES tanks were used for AMTP's ASTEP system to fulfil its thermal temperature requirement at high latitude location.

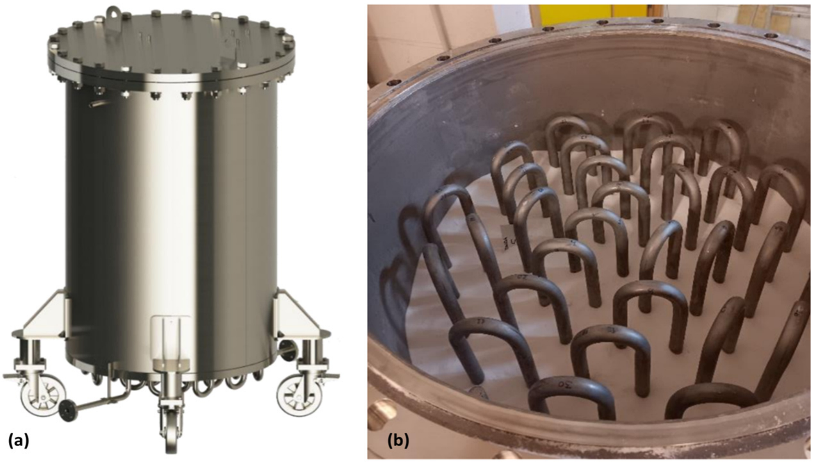

Figure 4. Thermal Energy Storage (**a**) TES tank and (**b**) multi-tubes & charged PCM inside TES tank [7] (Reproduced with permission of the first author of the conference paper).

1.1.3. Controls

The Control System (CS), which is the third part of the ASTEP system (Figure 1), is based on a Programmable Logic Control (PLC) unit and will ensure that the heat supply remains within the process specifications. This will be achieved through centralised control and flexible operation of the system [5]. The Control System will manage the signals from the sensors and perform the appropriate sequence in order to send commands to the actuators. The system will also have a user Control interface where the operator will be able to check in real-time the condition of the system and intervene when required. The PLC unit will transmit data throughout the system and the sensors and actuators will send and receive signals from the PLC to ensure the smooth operation of the ASTEP system. The CS is used by both end users, MAND and AMTP.

2. Methodology

The economic impact of the ASTEP system was conducted through life cycle costing (LCC) using SimaPro 9.2 software (Pre-Sustainability, The Netherlands) and the Ecoinvent 3.6 database (Ecoinvent, Zurich, Switzerland). In addition, the capital expenditure (CAPEX), levelised cost of energy (LCOE), energy cost savings, EU cost savings and benefit–cost ratio (BCR) of the ASTEP system were calculated using Excel 2021 software (Microsoft, Washington, DC, USA).

2.1. Life Cycle Costing of ASTEP System

The life cycle costing of ASTEP is the costs incurred during its lifetime from the manufacturing phase all the way through to its end-of-life disposal phase. It includes the costs of the components, labour, transportation, operational and maintenance and disposal costs of the ASTEP system. The life cycle costing (LCC) method in SimaPro 9.2 software was used for the economic assessment of the ASTEP system.

In general, LCC follows the four phases of ISO 14040/44 [14,15]:

(i). Goal and Scope of Study;
(ii). Life Cycle Inventory (LCI) Analysis;
(iii). Life Cycle Costing Impact Assessment;
(iv). Interpretation of Results.

2.2. Goal and Scope of the Economic Assessment of ASTEP System

The aim of this study is to conduct a comprehensive economic assessment of the ASTEP system, which provides thermal energy to industrial processes. The goal of the assessment is to quantify and evaluate the economic performance of the ASTEP system throughout its life cycle for each end-user, MAND and AMTP. The intended audience is industries that may use the ASTEP system. The functional unit of the ASTEP system is 1 kWh of thermal energy. The ASTEP system is a Fresnel solar thermal technology and has an estimated lifespan of 30 years [16]. The ASTEP system will provide a total of 27.8 MWh of annual thermal energy for each end user, MAND and AMTP, and this is based on the analytic models of Abbas et al. [13], which considers the climate model of Greece and Romania. The high-latitude SunDial design enables the SunDial to achieve the same energy production of 27.8 MWh at a high latitude of 47.1 °N as it does at a low latitude of 37.9 °N [13]. The system boundaries of the ASTEP system are presented in Figure 5 and cover the manufacturing of the materials/components, transportation of materials and components, operation and maintenance and disposal of the system. Therefore, the system boundaries of the LCC of the ASTEP system include the component costs, labour costs to manufacture and install the ASTEP system, transportation costs, operation and maintenance cost of the system and cost of dismantling and disposal of the components of the ASTEP system at its end of life stage.

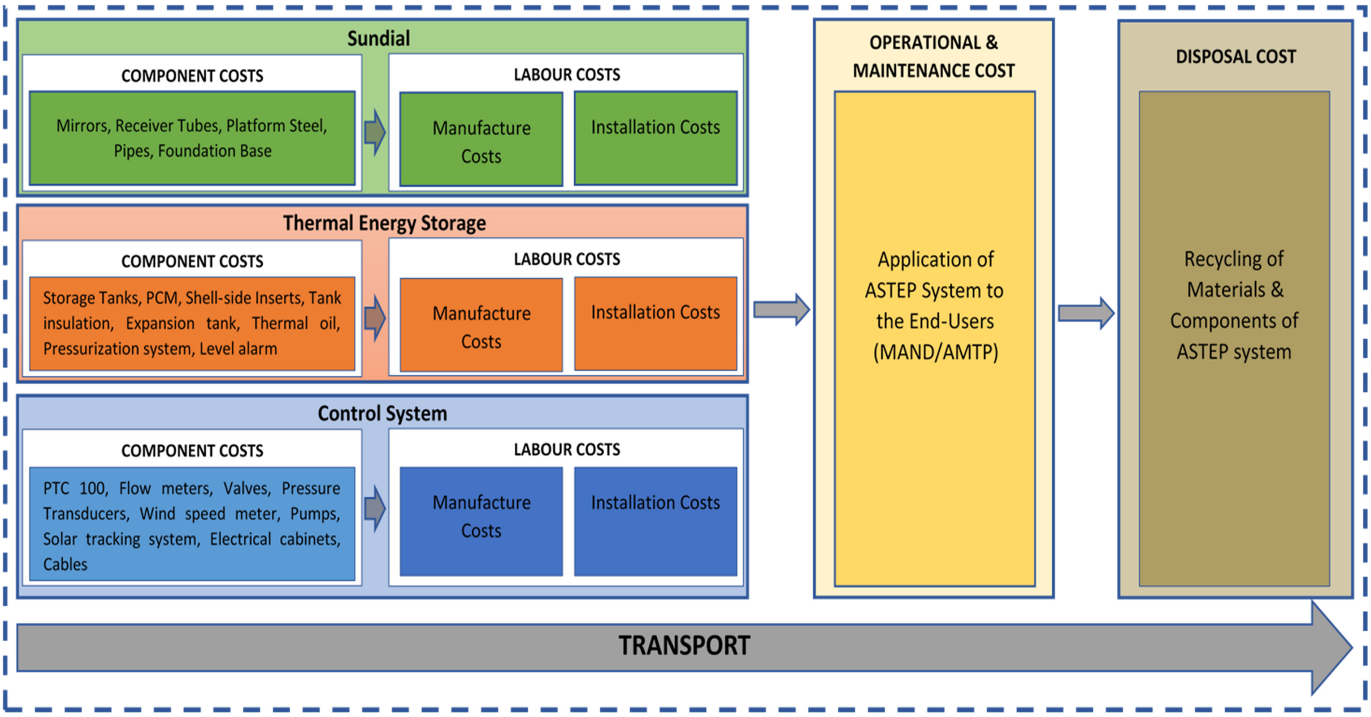

Figure 5. System boundaries of ASTEP.

2.3. Life Cycle Cost Inventory of the ASTEP System

Table 1 is the life cycle cost inventory list of ASTEP for MAND and AMTP. It consists of the SunDial, TES and Controls components, along with their associated costs for each end user, MAND and AMTP. The component costs for the SunDial, TES and Controls were provided by the project partners. The Life Cycle Inventory (LCI) cost data in Table 1 was used to perform LCC in SimaPro 9.2 software. The LCC method consists of the following sections: Characterisation, Damage and Weighting. The LCC method in SimaPro was used for each subsystem of ASTEP: SunDial, TES and Controls. In the Characterisation section, the impact category includes the component costs, labour, transportation, operation and maintenance and disposal costs for each subsystem of ASTEP. For the impact category of component costs for the SunDial, the list of SunDial components was placed alongside their costs per unit. To assign the component costs, the processes used in the manufacturing of the components as defined in the environmental assessment of ASTEP conducted through the Eco-invent database were selected. Then, the component costs were applied to these processes. For the labour impact category, the labour costs for the SunDial were added. Likewise, for the transportation, operation and maintenance (O&M) and disposal impact categories, the transportation cost, O&M and disposal costs for the SunDial were added. In the damage category, all the impact categories were assigned as variable costs with a factor of 1 applied to them, which means that the same currency was used for all of them, which was Euros. In the Weighting section, the variable costs were assigned a nominal discount rate of 7.5% and 6% used for renewable energy projects in Romania and Greece, respectively [17], and is used in the calculation of the LCC of the ASTEP system in SimaPro. The same process was applied for the TES and Controls of ASTEP for each end user.

Table 1. Component costs of ASTEP system (MAND and AMTP).

Components	Number of Components		Total Cost of Components (EUR)	
	MAND	AMTP	MAND	AMTP
SunDial Components				
Mirrors	4	6	3570	3130
Receiver Tubes	4	4	6944	6944
Platform Steel	1	1	4666	3478
Pipes	n/a	n/a	1927	1927
Foundation Base	1	1	9451	5264
TES Components				
Storage Tanks	1	2	24,555	49,110
Wheels	4	8	920	1840
Phase Change Materials	n/a	n/a	2072.4	4144.8
Shell-side Inserts	305	610	3690.5	7381
Tank Wall Insulation	n/a	n/a	5411	10,822
Expansion Tank and 7A Pipping	n/a	n/a	13,775	13,775
Thermal Oil	n/a	n/a	1833	2300
Level Alarm	1	1	265	265
Pressurisation System	1	1	413.83	431.83
Control Components				
PTC 100 (Temperature Sensors)	6	6	1037.1	1037.1
Flow Metres	2	2	4380	4380
3-w Valves	2	3	2666.08	3999.12
Pressure Transducers	2	2	720	720
Wind Speed Metre	1	1	150	150
SunDial Pump	1	1	1345.72	1345.72
Main Pump	1	1	636.89	636.89
Recirculation Pump	1	1	489.23	489.23
Mirror Tracking motor	0	6	0	7575.6
Platform Tracking System	2	2	2350	2350
Electrical Cabinet	1	1	9000	9000
Electrical Cables	n/a	n/a	1500	1500

2.4. Estimated Operational Expenses (OPEX) of ASTEP System

The OPEX of a solar thermal system includes the water and labour costs of cleaning the mirrors of the solar thermal system, the costs of replacing the heat transfer fluid, broken receivers and reflector mirrors, as well as the cost of energy to run the pumps, motors and Controls of the system [18]. This is because the mirrors of the solar thermal system must be cleaned periodically and the heat transfer fluid can also leak over time; hence, it may need to be replaced. The pumps, motors and the Controls of the solar thermal system may need electricity to function; hence, energy will be consumed. Old or broken components will need to be replaced as the solar thermal system is used over a period of time. All of these costs constitute the operation and maintenance costs of the ASTEP system. The OPEX percentage ratio calculated from the OPEX costs and total plant cost in Corona et al. [4] was 4.4% of the total plant cost, which included water and energy costs of running the solar thermal plant, replacement costs of components, management and administrative expenses regarding the operation and maintenance of the plant. This study uses 4.4% of the total capital cost as the estimated annual OPEX cost of the ASTEP system. The estimated OPEX of ASTEP is shown in Table 2.

Table 2. Estimated operational expenses (OPEX), transport, labour and dismantling and disposal (D&D) costs.

Estimated Annual OPEX (EUR)		**Estimated Transport Cost (EUR)**		**Estimated Labour Cost (EUR)**		**Estimated D&D Cost (EUR)**	
MAND	**AMTP**	**MAND**	**AMTP**	**MAND**	**AMTP**	**MAND**	**AMTP**
4565.8	6335.8	5984.8	6923.8	40,469.8	56,158.5	3113	4320

2.5. Estimated Transport, Labour and Disposal Costs of ASTEP System

The estimated transportation costs of the ASTEP system for each end-user are presented in Table 2. The transportation costs for the SunDial and TES of the ASTEP system were estimated as 3% of the equipment costs, as used by Corona et al. [4] in the life cycle costing of a solar thermal plant. The estimated transportation costs for the Controls were provided by the project partner responsible for the Controls of the ASTEP system.

The labour costs include the costs of personnel in the designing, constructing and installation of the ASTEP system. Corona et al. [4] was the only study in the reviewed literature that conducted a full life-cycle costing (LCC) of a solar thermal plant. The labour percentage ratio was calculated using data from Corona et al. [4] by dividing the total plant cost by its total labour cost (personnel, engineering management and project development costs), resulting in 39% of the total plant cost. This percentage was then used to estimate the labour costs of the ASTEP system. The dismantling and disposal (D&D) costs include the dismantling of the ASTEP system at its end-of-life stage. The D&D percentage ratio was obtained by dividing the total plant costs by the D&D costs provided by Corona et al. [4], resulting in 3% of the total plant cost. This percentage was used in estimating the D&D costs of the ASTEP system. The total estimated labour, OPEX, transport and D&D costs of the ASTEP system are presented in Table 2.

2.6. Calculation of the Life Cycle Cost (LCC), Capital Expenditure (CAPEX), Levelised Cost of Energy (LCOE) and Benefit–Cost Ration (BCR) of ASTEP

This section presents the calculations of the LCC, CAPEX, LCOE and BCR of ASTEP.

2.6.1. Calculation of the Life Cycle Cost of the ASTEP System

The LCC is the sum of the initial capital costs and the annual net present value costs accumulated during the lifespan of a project or technology. The LCC of ASTEP was calculated using the life cycle costing method in SimaPro 9.2 software.

2.6.2. Calculation of the CAPEX and LCOE of ASTEP System

This section presents the calculation of the CAPEX and LCOE of the ASTEP system.

$$\text{CAPEX} = \text{Total Component Cost} + \text{Labour Costs} \tag{1}$$

$$LCOE = \frac{\text{LCC}}{\sum_{n=1}^{N} \frac{\text{OE}_n}{(1 + \text{NDR})^n}} \tag{2}$$

Equation (1) was used to calculate the CAPEX by adding the total component costs and the labour costs of the ASTEP system. Equation (2) was used to calculate the LCOE of the ASTEP system. The LCOE is the cost of energy generated by renewable energy technologies and is one of the most popular financial metrics employed in the economic assessment of solar thermal plants [11,19–21]. The LCOE is the total net present value of all the expenditures over the lifespan of a solar thermal plant divided by the total generated energy. The LCOE cannot be calculated in SimaPro software; therefore, it was calculated in Excel. LCC is the life cycle cost, OE is the annual energy output of the system, NDR is the nominal discount rate and N is the lifespan of the solar thermal system [22]. The annual energy output used for the ASTEP system is 27.8 MWh for each end-user, MAND and AMTP [13]. The nominal discount rate is 6% for MAND and 7.5% for AMTP. The LCC, annual energy output, life span and nominal discount rate of the ASTEP system for MAND and AMTP were placed into Equation (2) in Excel to obtain their LCOE.

2.6.3. EU Carbon Cost Savings (MAND and AMTP)

The EU emissions trading system (ETS) was established in 2005 as the world's first carbon market. Its goal is to limit GHG emissions from polluting installations by placing a price on carbon, thereby incentivising companies to reduce their emissions [23]. The EU ETS works on a 'cap and trade' system. A cap is set on the total amount of GHG that can be emitted by the installations covered by the system. The cap is reduced annually in line with the EU's climate target, ensuring that emissions are reduced over time. Every year, companies must surrender enough allowances to fully account for their emissions; otherwise, heavy fines are imposed. If a business reduces its emissions, it can either keep the spare allowances to use in the future or sell them [24]. Therefore, MAND and AMTP can sell their spare emission allowances saved by the ASTEP system. If they were to sell their spare allowances over the period of 30 years at the same price as the carbon price, this would double their EU carbon cost savings.

The methodology used to forecast future EU carbon prices up to 2044 is based upon the POLES-Enerdata model, which uses the EU ETS and Market Stability Reserve (MSR) data to make its projections. The aim of the MSR is to provide stability to the EU ETS market by controlling the number of emission allowances in the system. The number of emission allowances present in the system is calculated each year. If this number is greater than the ceiling value, the volume of emission allowance for the following year is reduced. If the volume is below the floor value, then some emission permits are reinjected from the reserve [25]. In the POLES-Enerdata model, a carbon price is established that encourages businesses and industries to reduce their emissions by making fossil fuels and carbon-emitting technologies less competitive. The EU-ETS and the MSR are used in the POLES-Enerdata model to quantify the projected EU carbon prices up to 2044 [25].

There were no projected EU carbon prices found for 2045–2049; therefore, the projected EU carbon price for 2044 was used for 2045–2049. The forecasted global carbon price of EUR 519/tCO_2 for 2050 was then used for 2050–2053 [26]. The EU carbon cost savings of the ASTEP system, when applied to MAND and AMTP's processes, was calculated by multiplying the forecasted annual EU carbon price by the annual GHG emission savings of MAND and AMTP's ASTEP systems for a period of 30 years from 2024 to 2053.

2.6.4. Energy Cost Savings (MAND and AMTP)

The forecasted electricity prices for Europe for 30 years, from 2024 to 2053, were used in the calculation of the energy cost savings for Greece and Romania [27]. There were no forecasted LPG prices for Europe or Greece; therefore, logarithmic regression was conducted in Excel software using the historic LPG prices for Greece from 2014 to 2024 to forecast future LPG prices for Greece from 2025 to 2053 [28]. The forecasted electricity and LPG prices were used to calculate the energy cost savings of MAND and AMTP when the ASTEP system is applied to their processes. It is estimated that half of the energy of the ASTEP system is used to provide heating and the other half is used to provide cooling for MAND's processes, which equates to 13.9 MWh for the heating and 13.9 MWh for the cooling processes of MAND. MAND uses LPG for its heating processes and electricity for its cooling processes. The inflation rate for 2024–2029 for Greece and Romania was obtained from Statista [29,30]. There was no forecasted inflation rate found for Greece and Romania for 2030–2053; therefore, logarithmic regression was conducted in Excel software using the historic inflation rates for Greece and Romania to forecast future inflation rates for Greece and Romania for 2030–2053. The forecasted annual electricity and LPG prices for Greece and Romania were then multiplied by the annual energy provided by the ASTEP system, which is 27.8 MWh, to obtain the energy cost savings of MAND and AMTP.

2.6.5. Calculation of Electricity Cost Savings for MAND and AMTP

This section presents the calculation of the estimated electricity cost savings for each end-user, MAND and AMTP, for a period of 30 years from 2024 to 2053.

$$\text{Forecasted Annual Electricity Cost} = \text{Energy Consumed} \times \text{Forecasted Annual Electricity Rate} \tag{3}$$

$$\text{Total Electricity Cost Savings} = \sum_{n=1}^{30} [(\text{Forecasted Annual Electricity Cost}) \times (1 + r)] \tag{4}$$

Equation (3) shows the calculation for the forecasted annual electricity cost based on the annual electricity consumption that the ASTEP system will replace at each end-user, MAND and AMTP. The ASTEP system will be used to replace annual electricity consumption of 27.8 MWh for AMTP's processes and 13.9 MWh for MAND's processes. This amount is then multiplied by the forecasted average EU electricity rate for each year up to 2053. In Equation (4), the forecasted annual electricity cost is multiplied by the annual inflation rate (r) for Greece and Romania to obtain the total electricity cost savings for MAND and AMTP over a period of 30 years from 2024 to 2053.

2.6.6. Calculation of LPG Cost Savings for MAND

This section presents the calculation of the estimated LPG cost savings for MAND when the ASTEP system is applied to their processes for a period of 30 years from 2024 to 2053.

$$\text{Forecasted Annual LPG Cost} = \text{LPG consumed} \times \text{Forecasted Annual LPG Rate} \tag{5}$$

$$\text{Total LPG Cost Savings} = \sum_{n=1}^{30} [(\text{Forecasted Annual LPG Cost}) \times (1 + r)] \quad (6)$$

Equation (5) shows the calculation for the forecasted annual LPG cost based on the annual LPG consumption that the ASTEP system will replace at MAND, which is 1963.3 L of LPG each year. This amount is then multiplied by the forecasted annual average LPG rate for Greece each year up to 2053. In Equation (6), the forecasted annual LPG cost is multiplied by the annual inflation rate (r) for Greece from 2024 to 2053 to obtain the total LPG cost savings for MAND over a period of 30 years.

2.6.7. Calculation of Total Energy Cost Savings and EU Carbon Cost Savings

This section presents the calculation of the total energy cost savings and EU carbon cost savings achieved when the ASTEP system is used to provide thermal energy to their MAND And AMTP processes for a period of 30 years. Equation (7) is used to calculate the total energy cost savings of MAND's ASTEP system by adding its total electricity and LPG cost savings. Equation (8) is used to calculate the EU carbon cost savings where the annual carbon emissions saved by the ASTEP system for each end user are multiplied by the annual EU carbon price for a period of 30 years from 2024 to 2053.

$$\text{Total Energy Cost Savings} = \text{Total Electricity Cost Savings} + \text{Total LPG Cost Savings} \quad (7)$$

$$\text{EU Carbon Cost Savings} = \sum_{n=1}^{30} (\text{Annual Carbon Emissions Saved} \times \text{Forecasted EU Carbon Price}) \quad (8)$$

2.6.8. Calculation of Total Financial Savings and Benefit–Cost Ratio (MAND and AMTP)

This section presents the calculation of the total financial savings and benefit–cost ratio achieved by each end-user, MAND and AMTP, when the ASTEP system is applied to their industrial processes for 30 years. Equation (9) is used to calculate the total financial savings for each end user, MAND and AMTP. The total EU carbon cost savings is multiplied by 2 because by using the ASTEP system, which is a renewable technology, to provide energy for industrial processes, the organisation avoids paying the EU carbon costs that would have been applied if fossil fuel (grid electricity, natural gas or LPG) had been used for their processes. If an organisation reduces its emissions, the EU Emission Trading System (ETS) allows the organisation to either keep the spare allowances to use in the future or to sell them. Therefore, MAND and AMTP can choose to sell their spare allowances, which will result in double EU carbon cost savings. Equation (10) is used to calculate the benefit–cost ratio of MAND and AMTP's ASTEP systems over their lifespan of 30 years.

$$\text{Total Financial Savings} = \text{Total Energy Cost Savings} + (\text{EU Carbon Cost Savings} \times 2) \quad (9)$$

$$\text{Benefit–Cost Ratio} = \text{Total Financial Savings} \div \text{Life Cycle Cost} \quad (10)$$

3. Results and Discussion

This section presents and discusses the economic assessment results of the ASTEP system for MAND and AMTP. This includes the CAPEX, LCC, LCOE, energy cost savings, EU cost savings and BCR of the ASTEP system for both end-users.

3.1. CAPEX, LCC and LCOE of ASTEP System (MAND and AMTP)

This section presents the results of the CAPEX, LCC and LCOE of the ASTEP system for both end-users. Figure 6 shows the CAPEX of the ASTEP system, which is EUR 144,238.6 for MAND and EUR 200,154.8 for AMTP. Figures 7 and 8 show the LCC and LCOE of the ASTEP system, respectively. It can be seen in Figures 6–8 that the CAPEX, LCC and

LCOE of AMTP's ASTEP system are greater than that of MAND. This was due to its higher component and labour costs, which can be attributed to AMTP's greater thermal temperature requirement of 230 °C at a high latitude, requiring a unique design of its ASTEP system compared to MAND. AMTP's ASTEP system required a double-axis solar tracking system to track the sun, absorbing more of its solar irradiance to achieve its high thermal temperature for its processes. Furthermore, two TES tanks were needed to fulfil AMTP's thermal energy requirement. In contrast, MAND, which requires a lower thermal temperature of 175 °C for its processes, is located at low latitudes and receives high solar irradiance. Therefore, a single-axis solar tracking system and only one TES tank were used for MAND's ASTEP system, which contributed to its lower component cost compared to AMTP. The results suggest that solar thermal systems located at sites with low latitude and high solar irradiance are likely to have lower component costs than those installed at sites of high latitude and low solar irradiance. This is supported by results in the reviewed literature, which showed that the CAPEX of the solar thermal power plants was lower at locations with high solar irradiance and higher at locations with low solar irradiance [4,18].

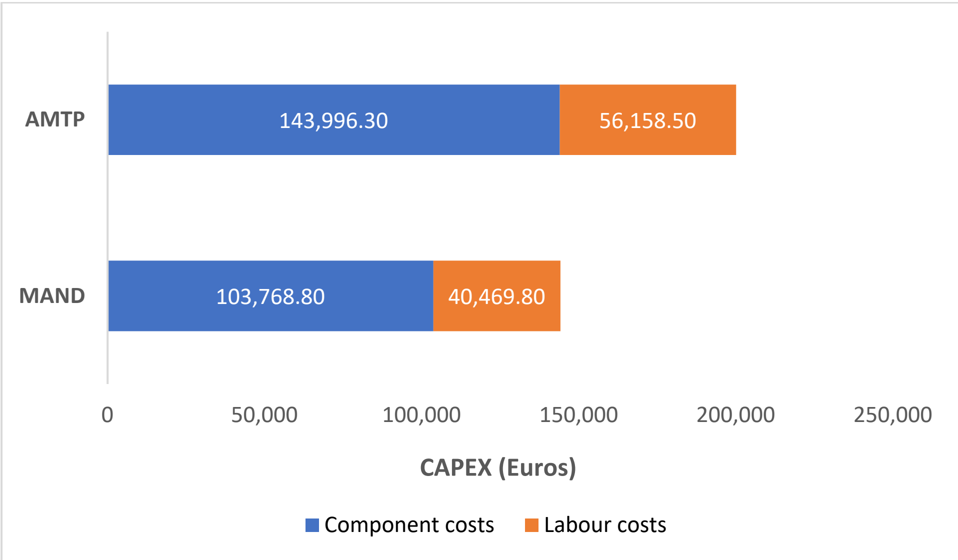

Figure 6. CAPEX of ASTEP system (MAND and AMTP).

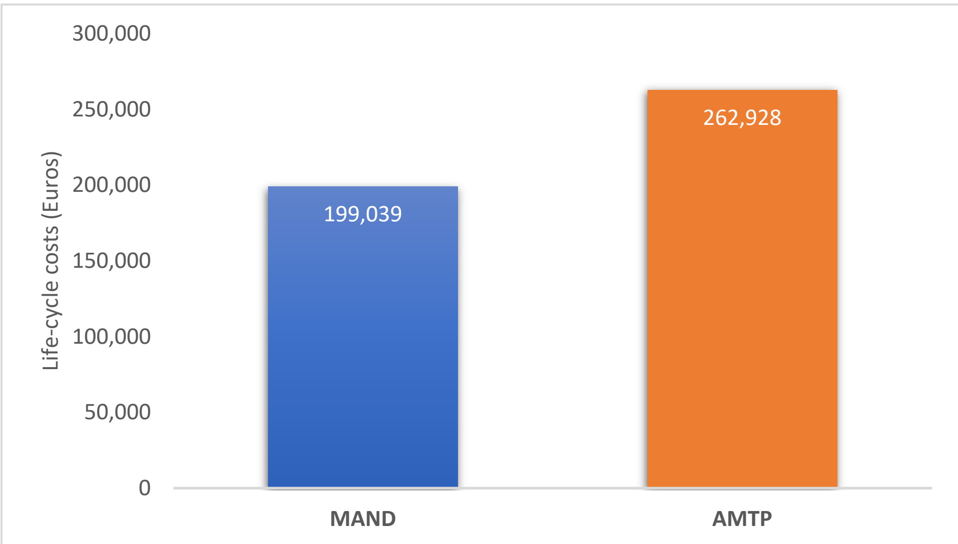

Figure 7. Life cycle cost of ASTEP system (MAND and AMTP).

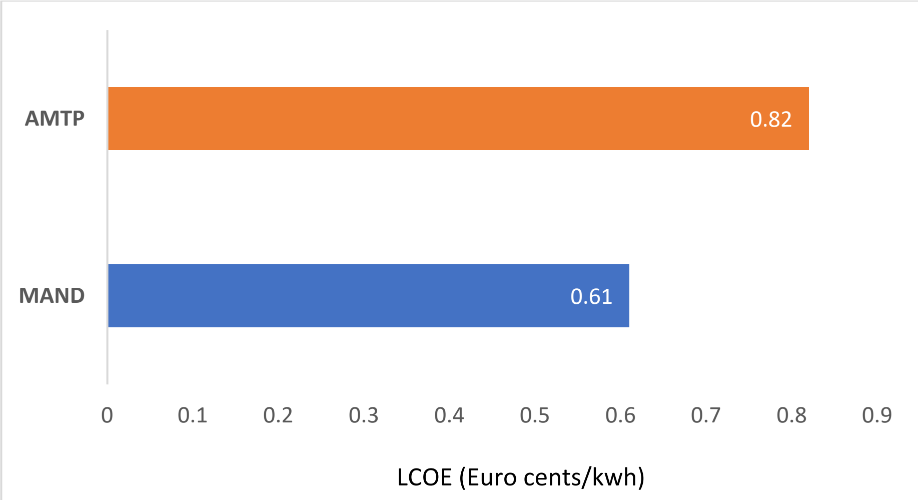

Figure 8. LCOE of ASTEP system (MAND and AMTP).

The CAPEX of a plant has a strong influence on its LCC and LCOE. This has been confirmed by studies that found that the CAPEX can constitute up to four-fifths of the entire cost of a solar thermal project, thereby having a great impact on the LCC and LCOE of the plant [31,32]. Most of the studies in the reviewed literature assessed the economic performance of mainly PT and ST plants using LCOE, with only a few studies assessing LFR plants. In addition, the majority of these studies focussed on solar thermal power plants with large capacities of 50 MW and above that generated electricity, while only a limited number of studies assessed plants generating steam or thermal energy [33,34]. After a thorough literature review, no study was found that computed the LCOE or LCC of an LFR plant used for producing thermal energy. Therefore, to the best of the authors' knowledge, this is the first study that has calculated the LCOE and LCC of an LFR plant, in particular a rotary Fresnel system, used for generating thermal energy for industrial processes.

3.2. Energy Cost Savings (MAND and AMTP)

The electricity cost savings of MAND and AMTP when thermal energy from the ASTEP system is used to replace some of their grid electricity consumption for their processes is calculated using Equations (3) and (4). The LPG cost savings of MAND when thermal energy from the ASTEP system is used to replace some of its LPG consumption is calculated using Equation (6). It can be seen in Table 3 that when the ASTEP system is applied to the processes of the end-users, AMTP's energy cost savings are greater than MAND. This is because all the energy (27.8 MWh) produced by the ASTEP system was used for the heating demand of AMTP's process. In contrast, half of the energy (13.9 MWh) of MAND's ASTEP system was used for some of their heating demand, and the other half was used for some of the cooling demand of their processes. MAND uses LPG and electricity to meet the heating and cooling demands of their processes, respectively. The results in Table 3 show that when electricity and LPG consumption is replaced by thermal energy supplied by the ASTEP system, the system provides total energy cost savings of EUR 110,054 for MAND and EUR 143,827 for AMTP over a period of 30 years.

Table 3. Energy cost savings (MAND and AMTP).

MAND's Energy Cost Savings			AMTP's Energy Cost Savings
Electricity	LPG	Total	Electricity
EUR 47,936	EUR 62,118	EUR 110,054.4	EUR 143,827

3.3. EU Carbon Cost Savings (MAND and AMTP)

The EU carbon cost savings of the ASTEP system when applied to MAND and AMTP's industrial processes over a period of 30 years was calculated using Equation (8). It can be seen from the results in Table 4 that MAND achieved higher EU carbon cost savings than AMTP. This was due to the higher annual GHG emissions reduction achieved by MAND's ASTEP system as the carbon intensity of grid electricity in Greece is higher than in Romania.

Table 4. EU Carbon Cost Savings (MAND and AMTP).

	Annual GHG Emissions Reduction (Tonnes of CO_2 Equivalent)	**EU Carbon Cost Savings (EUR)**
MAND	9.7	69,596.72
AMTP	8.3	59,551.84

3.4. Total Financial Savings of ASTEP System (MAND and AMTP)

The total financial savings of the ASTEP system when applied to MAND and AMTP's industrial processes are presented in Table 5. The total financial savings consist of the energy and EU carbon cost savings over a period of 30 years, which is the estimated lifespan of the ASTEP system. According to the rules of the EU ETS, MAND and AMTP can avoid paying the EU carbon costs by using a renewable energy system such as the ASTEP system to provide thermal energy for their processes instead of fossil fuel (grid electricity, natural gas or LPG). If an organisation reduces its emissions, the EU ETS allows it to either keep the spare allowances to use in the future or to sell them. Therefore, MAND and AMTP can choose to sell their spare allowances, which will result in double EU carbon cost savings. Therefore, the EU carbon cost savings for MAND and AMTP have been doubled, as it is assumed that MAND and AMTP will sell their spare allowances. It can be seen that AMTP's ASTEP system achieved higher total financial savings than MAND, which can be attributed to its higher energy cost savings. The results in Table 5 show that the ASTEP system provides significant economic benefits to MAND and AMTP when it is used to replace electricity and LPG consumption in their industrial processes over a period of 30 years.

Table 5. Total financial savings of ASTEP system (MAND and AMTP).

	MAND	**AMTP**
Energy Cost Savings	EUR 110,054.4	EUR 143,827
EU Carbon Cost Savings	EUR 139,193.44	EUR 119,103.68
Total Financial Savings	EUR 249,247.84	EUR 262,930.68

3.5. BCR of ASTEP System (MAND and AMTP)

The BCR is used to assess the economic feasibility of a project or technology and to determine whether and to what extent its benefits outweigh its costs. This ratio is calculated as the total present value of benefits divided by the total present value of costs [18]. A BCR value greater than 1 means that the system's financial benefit is higher than its cost and is therefore profitable. A BCR value of 1 means the system's financial benefit is equal to its costs and, therefore, the system breaks even. MAND's ASTEP system is more profitable than AMTP's ASTEP system as it achieved a BCR of 1.25 compared to 1 for AMTP. AMTP's ASTEP system achieved higher financial savings than MAND; however, its higher LCC resulted in it having a lower BCR than MAND's ASTEP system. This shows the importance of reducing the LCC of a solar thermal plant in order to improve its profitability. The results from this study indicate that solar thermal systems located in high-latitude regions with low solar irradiance are likely to be more expensive resulting in lower BCR values and less profitability than plants located in low-latitude regions with high solar irradiance.

There were limited studies in the reviewed literature that used the BCR metric to assess the economic performance of solar thermal plants. This is confirmed by Gobio-Thomas et al. [11], who investigated the economic assessment of solar thermal plants and found that BCR was one of the least used metrics in the financial evaluation of solar thermal plants. There were only two studies found that used BCR in the financial assessment of solar thermal plants and these were based on ST and PT plants used for electricity generation [18,35]. There were no studies that calculated the BCR of a linear or rotary Fresnel plant used to generate thermal energy. Therefore, to the best of the authors' knowledge, this is the first study that has calculated the BCR of a rotary Fresnel solar thermal system used to produce thermal energy for industrial processes at different latitudes.

4. Conclusions

The economic assessment of a novel solar thermal technology, ASTEP, was conducted for its two end-users located at different latitudes. The results revealed that AMTP's ASTEP system had higher capital costs, LCC and LCOE, than MAND, which was mainly due to AMTP's high-latitude location, resulting in lower solar irradiance than MAND. This led to AMTP's ASTEP system requiring a different design, which was more expensive than the design of MAND's system. The results of this study suggest that solar thermal systems located at sites with high latitude and low solar irradiance such as AMTP are likely to have higher CAPEX than those installed at sites of low latitude and high solar irradiance, such as MAND. This is supported by results in the reviewed literature, which showed that the CAPEX of the solar thermal plants was lower at locations with high solar irradiance but greater at locations with low solar irradiance.

The BCR measures the profitability or economic feasibility of a product or project. MAND's ASTEP system achieved a BCR of 1.25, making it profitable, while the BCR of AMTP's ASTEP system is 1, meaning the system breaks even. MAND's ASTEP system's higher BCR can be attributed to its lower LCC than AMTP. Therefore, reducing the LCC of AMTP's ASTEP system could increase its BCR value and improve its profitability. The energy cost savings achieved by MAND and AMTP's ASTEP systems were EUR 110,054 and EUR 143,827, respectively. The EU carbon cost savings of the ASTEP system when used to supply thermal energy to the industrial processes were EUR 139,193 for MAND and EUR 119,104 for AMTP. This resulted in total financial savings of EUR 249,248 and EUR 262,931 for MAND and AMTP's ASTEP system, respectively, over a period of 30 years. This shows the significant financial benefits of the ASTEP system for industries through its energy and EU carbon cost savings, which can encourage businesses to use the ASTEP system instead of fossil fuels to provide thermal energy for their processes, leading to greater environmental sustainability and economic savings. The key contribution of this research is that it is the first study, to the best of the authors' knowledge, to assess the economic performance of a rotary Fresnel solar thermal system that supplies sustainable thermal energy above 150 °C to industries. This study shows that the ASTEP system can provide economic benefits to industries in high- and low-latitude regions, while contributing to their environmental sustainability.

Author Contributions: Conceptualisation, A.R. and V.S.; methodology, L.G.-T.; formal analysis, L.G.-T.; investigation, L.G.-T.; data curation and resources, R.A., M.B., J.P.S., A.T., K.N. and P.K.; writing—original draft preparation, L.G.-T.; writing—review and editing, L.G.-T. and V.S.; visualisation, L.G.-T.; supervision, M.D. and V.S.; project administration, A.R. and V.S.; funding acquisition, A.R. and V.S. All authors have read and agreed to the published version of the manuscript.

Funding: The authors declare that this project is funded by the EU Horizon 2020 research and innovation programme, Application of Solar Energy in Industrial Processes (ASTEP), grant agreement number 884411. The funder was not involved in the study design, collection, analysis, interpretation of data, the writing of this article or the decision to submit it for publication.

Institutional Review Board Statement: Not Applicable.

Informed Consent Statement: Not Applicable.

Data Availability Statement: Data used in this study are available from the corresponding author upon request.

Conflicts of Interest: Author Albert Torres was employed by the company IRIS Technology. Author Peter Kew was employed by the company David Reay & Associates. All authors declare that the research was conducted in the absence of any commercial or financial relationships that could be construed as a potential conflict of interest.

References

1. UNFCCC. The Paris Agreement. Available online: https://unfccc.int/process-and-meetings/theparis-agreement (accessed on 2 October 2024).
2. European Commission. Delivering the European Green Deal. Available online: https://commission.europa.eu/strategy-and-policy/priorities-2019-2024/european-green-deal/delivering-european-green-deal_en (accessed on 2 October 2024).
3. Gobio-Thomas, L.B.; Darwish, M.; Stojceska, V. Environmental impacts of solar thermal power plants used in industrial supply chains. *Therm. Sci. Eng. Prog.* **2023**, *38*, 101670. [CrossRef]
4. Corona, B.; Cerrajero, E.; López, D.; San Miguel, G. Full Environmental Life Cycle Cost Analysis of Concentrating Solar Power Technology: Contribution of Externalities to Overall Energy Costs. *Sol. Energy* **2016**, *135*, 758–768. [CrossRef]
5. Rovira, A.; Enriquez, J.; Abbas, R.; Montes, M.J.; Barbero, R.; Cavero, G.; Solano, J.P.; Herrero-Martín, R.; Reay, D.; Piaton, G.; et al. ASTEP: Application of Solar Thermal Energy to Processes, 2020. In Proceedings of the SolarPACES Conference, Online, 28 September–2 October 2020. Available online: https://zenodo.org/records/5772839 (accessed on 3 November 2024).
6. ASTEP Project. Objectives. Available online: https://astepproject.eu/objectives/ (accessed on 13 November 2024).
7. Muñoz-Cámara, J.; Zitouni, R.; Díaz-Moreno, L.; Solano, M.A.; Bensaad, S.B.; Pérez-García, J.; Solano, J.P. Solidification and melting characteristics of an enhanced LTES system for solar heat in industrial processes. In Proceedings of the 13th National and 4th International Conference in Engineering Thermodynamics, Castellón de la Plana, Spain, 29 November–1 December 2023.
8. Banacloche, S.; Herrera, I.; Lechón, Y. Towards energy transition in Tunisia: Sustainability assessment of a hybrid concentrated solar power and biomass plant. *Sci. Total Environ.* **2020**, *744*, 140729. [CrossRef] [PubMed]
9. Hirbodi, K.; Enjavi-Arsanjani, M.; Yaghoubi, M. Techno-economic assessment and environmental impact of concentrating solar power plants in Iran. *Renew. Sustain. Energy Rev.* **2020**, *120*, 109642. [CrossRef]
10. Aseri, T.K.; Sharma, C.; Kandpal, T.C. Estimation of Capital Costs and Techno-Economic Appraisal of Parabolic Trough Solar Collector and Solar Power Tower Based CSP Plants in India for Different Condenser Cooling Options. *Renew. Energy* **2021**, *178*, 344–362. [CrossRef]
11. Gobio-Thomas, L.B.; Abbas, R.; Darwish, M.; Stojceska, V. Review on the economic impacts of solar thermal power plants. *Therm. Sci. Eng. Prog.* **2023**, *46*, 102224. [CrossRef]
12. Mihoub, S. Design, economic, and environmental assessments of linear Fresnel solar power plants. *Environ. Prog. Sustain. Energy* **2019**, *39*, 13350. [CrossRef]
13. Abbas, R.; Barbera, R.; Rovira, A.; Barnetche, M. Sundial, a new collector for solar heat for industrial processes: Optical and thermal design. *Therm. Sci. Eng. Prog.* **2023**, *44*, 102025. [CrossRef]
14. Klopffer, W.; Grahl, B. Life cycle assessment (LCA). In *A Guide to Best Practice*; Wiley: Weinheim, Germany, 2014. Available online: https://books.google.co.uk/books?id=NkRsAwAAQBAJ&dq=iso+14040/44+LCA+BEST+PRACTICES+environmental+management+systems&lr=&source=gbs_navlinks_s (accessed on 16 December 2023).
15. *ISO 14040*; Environmental Management—Life Cycle Assessment—Principles and Framework. ISO: Geneva, Switzerland, 2016.

16. Marugán-Cruz, C.; Serrano, D.; Gómez-Hernández, J.; Sánchez-Delgado, S. Solar multiple optimization of a DSG linear Fresnel power plant. *Energy Convers. Manag.* **2019**, *184*, 571–580. [CrossRef]
17. AURES. Renewable Energy Financing Conditions in Europe: Survey & Impact Analysis. 2021. Available online: https://www.isi.fraunhofer.de/content/dam/isi/dokumente/ccx/2021/AURES_II_D5_2_financing_conditions.pdf (accessed on 6 September 2024).
18. Krishnamurthy, P.; Mishra, S.; Banerjee, R. An Analysis of Costs of Parabolic Trough Technology in India. *Energy Policy* **2012**, *48*, 407–419. [CrossRef]
19. Zhuang, X.; Xu, X.; Liu, W.; Xu, W. LCOE Analysis of Tower Concentrating Solar Power Plants Using Different Molten-Salts for Thermal Energy Storage in China. *Energies* **2019**, *12*, 1394. [CrossRef]
20. Zhao, Z.; Chen, Y.; Thomson, J.D. Levelized cost of energy modeling for concentrated solar power projects: A China study. *Energy* **2017**, *120*, 117–127. [CrossRef]
21. Sultan, A.; Hughes, K.; Ingham, D.B.; Ma, L.; Pourkashanian, M. Techno-economic competitiveness of 50 MW concentrating solar power plants for electricity generation under Kuwait climatic conditions. *Renew. Sustain. Energy Rev.* **2020**, *134*, 110342. [CrossRef]
22. Shafiee, M.; Alghamdi, A.; Sansom, C.; Hart, P.; Encinas-Oropesa, A. A Through-Life Cost Analysis Model to Support Investment Decision-Making in Concentrated Solar Power Projects. *Energies* **2020**, *13*, 1553. [CrossRef]
23. Statista. Daily European Union Emission Trading System (EU-ETS) Carbon Pricing from January 2022 to September 2023. Available online: https://www.statista.com/statistics/1322214/carbon-prices-european-union-emission-trading-scheme/#:~:text=EU-ETS%20allowance%20prices%20in%20the%20European%20Union%202022-2023&text=The%20price%20of%20emissions%20allowances,of%20CO%E2%82%82%20in%20February%202023 (accessed on 3 November 2023).
24. European Commission. What Is the EU ETS? Available online: https://climate.ec.europa.eu/eu-action/eu-emissions-trading-system-eu-ets/what-eu-ets_en#a-cap-and-trade-system (accessed on 2 November 2024).
25. Enerdata. Carbon Price Forecast Under the EU ETS. Available online: https://www.enerdata.net/publications/executive-briefing/carbon-price-projections-eu-ets.html (accessed on 8 June 2024).
26. Network for Greening the Financial System (NGFS). NGFS Climate Scenarios for Central Banks and Supervisors. June 2021. Available online: https://www.ngfs.net/sites/default/files/medias/documents/ngfs_climate_scenarios_phase2_june2021.pdf (accessed on 12 June 2024).
27. Energy Brainpool, 2024. EU Energy Outlook 2060: How Will Power Prices, Generation and Demand Develop? Available online: https://blog.energybrainpool.com/en/eu-energy-outlook-2060-how-will-power-prices-generation-and-demand-develop/ (accessed on 25 November 2024).
28. MyLPGeu. Chart of Fuel Prices in Greece. Available online: https://www.mylpg.eu/stations/greece/prices/#chart (accessed on 19 November 2024).
29. Statista. Greece: Inflation Rate from 1988 to 2028. Available online: https://www.statista.com/statistics/276351/inflation-rate-in-greece/ (accessed on 3 November 2024).
30. Statista. Romania: Inflation Rate from 1988 to 2028. Available online: https://www.statista.com/statistics/373209/inflation-rate-in-romania/#:~:text=The%20average%20inflation%20rate%20in,to%202.5%20percent%20in%202028 (accessed on 5 November 2024).
31. Hinkley, J.T.; Hayward, J.A.; Curtin, B.; Wonhas, A.; Boyd, R.; Grima, C.; Tadros, A.; Hall, R.; Naicker, K. An Analysis of the Costs and Opportunities for Concentrating Solar Power in Australia. *Renew. Energy* **2013**, *57*, 653–661. [CrossRef]
32. Agyekum, E.B.; Velkin, V.I. Optimization and Techno-Economic Assessment of Concentrated Solar Power (CSP) in South-Western Africa: A Case Study on Ghana. *Sustain. Energy Technol. Assess.* **2020**, *40*, 100763. [CrossRef]
33. Backes, J.G.; D'Amico, A.; Pauliks, N.; Guarino, S.; Traverso, M.; Lo Brano, V. Life Cycle Sustainability Assessment of a Dish-Stirling Concentrating Solar Power Plant in the Mediterranean Area. *Sustain. Energy Technol. Assess.* **2021**, *47*, 101444. [CrossRef]
34. Dabwan, Y.N.; Pei, G.; Gao, G.; Li, J.; Feng, J. Performance Analysis of Integrated Linear Fresnel Reflector with a Conventional Cooling, Heat, and Power Tri-Generation Plant. Renew. *Energy* **2019**, *138*, 639–650. [CrossRef]
35. Lipu, M.S.H.; Jamal, T. Techno-economic Analysis of Solar Concentrating Power (CSP) in Bangladesh. *Int. J. Adv. Renew. Energy. Res.* **2013**, *2*, 750–762.